EURASIAN PHYSICAL TECHNICAL JOURNAL

2025, Volume 22, No.1 (51)

https://doi.org/10.31489/2025N1/115-126

Received: 25/09/2024 Revised: 18/02/2025 Accepted: 18/03/2025 Published online: 31/03/2025

Original Research Article

UDC: 524.7; 52; 52-16/-17; 520.88; 520.2/.8

SPECTRAL AND PHOTOMETRIC STUDIES OF MRK6 AND MRK1040 IN THE OPTICAL RANGE

Shomshekova S.A.*, Denissyuk E.K., Kondratyeva L.N.,
Serebryanskiy A.V., Aimanova G.K., Aktay L.

Fesenkov Astrophysical Institute, Almaty, Kazakhstan
*Corresponding author: shomshekova@fai.kz

Abstract. *This paper is dedicated to the study of variability in active galactic nuclei, which play a key role in understanding the physical processes occurring in their central regions. This research focuses on the analysis of photometric and spectral variability of two Seyfert galaxies, MRK 6 and MRK 1040, based on archival and modern observations. For the first time, the results of photometric observations of MRK 6 have been processed, with special attention given to the profiles of emission lines and the identification of additional spectral components that may indicate gas outflows. The velocity dispersions of each emission-line component have been determined for the studied galaxies. In some profiles of Hα and Hβ, their velocity dispersions and corresponding line-of-sight velocities have been estimated, which may indicate the outflow of matter from the central regions of the galaxies.*

Keywords: active galactic nuclei, Seyfert galaxies, photometry, spectroscopy, light curves, emission lines.

1. Introduction

This work is dedicated to the study of selected Seyfert galaxies from the Markarian list. Spectral and photometric studies of Seyfert galaxies from the Markarian list have been conducted at Fesenkov Astrophysical Institute (FAI) for several decades. A significant factor that has increased the efficiency of studies on active nuclei of poorly studied Seyfert galaxies is the implementation of an innovative spectral instrument developed at FAI in 2022. This instrument enables the acquisition of spectra from distant, hence faint and less studied Seyfert galaxies. Due to the large number of Seyfert galaxies discovered to date, both ground-based and space observatories dedicated to studying Active Galactic Nuclei (AGN) cannot cover all these Seyfert galaxies with systematic observations, which are crucial due to the unpredictable photometric and spectral variability of AGNs. Therefore, systematic observations and studies of poorly studied Seyfert galaxies remain a relevant task.

The paper [1] presents the results of a 22-year study of the galaxy MRK 6 using X-ray data from 2001 to 2022. Changes in the spectral and temporal behavior of the galaxy were detected in both X-ray and optical ranges. In another study [2], the morphology and kinematics of ionized gas in the galaxy MRK 6 were investigated, revealing extended filaments of ionized gas. Analysis of the kinematics and ionization state of gas in these filaments suggests that the hard radiation from the active nucleus illuminates externally accreted material, which rotates nearly perpendicular to the stellar disk of MRK 6. In the study [3], a new method is

presented for measuring the radius of the equatorial scattering region in Type 1 active galaxies using the polarization of broad lines, indicating a scattering region size of approximately 100 light-days in MRK 6. The kinematics of gas and emission line profiles of Hβ in active galaxies were investigated in the study [4]. Observations, exemplified by MRK 6, revealed complex structures, providing an opportunity to search for close binary supermassive black holes. In the study [5], the analysis of X-ray reverberation in six active galactic nuclei using Granger causality analysis was conducted. Granger causality delays and their variations over time were analyzed for each individual light curve. Significant delays correlating with the light curve were observed in all active galactic nuclei except MRK 1040. It is suggested that the spread of the obtained delays may be related to the expansion of the corona. It is suggested that in IZw1, MRK 704, and MRK 1040, the corona may be more compact. The paper [6] presents the results of high-resolution X-ray spectroscopy of warm absorption in the galaxy type MRK 1040. The observations were conducted from 2013 to 2014 with a total exposure of 200 ks. The spectrum revealed the presence of warm absorption, including absorption lines of Ne, Mg, and Si ions, as well as H-like lines of S and Ar. The profiles indicate low outflow velocities of the absorbing gas, which may suggest possible attenuation of outflowing gas on large scales in the galaxy MRK 1040. The results from all authors indicate the complexity and diversity of physical processes occurring in AGNs, contributing to a better understanding of the underlying mechanisms.

2. Photometric and spectral observations

Photometric observations of the studied objects at FAI have been conducted since 2015. The observations are carried out at the Tien Shan Astronomical Observatory (TShAO) using the Zeiss-1000 "East" telescope with a modified optical system and equipped with an Apogee Alta U9000 CCD camera, with a field of view of 20'×20'. Spectral observations were conducted using the AZT-20 telescope at the Assy-Turgen Observatory. This is the largest telescope in Kazakhstan, capable of detecting extremely faint objects (up to 21-22 stellar magnitudes). Currently, the AZT-20 is equipped with a spectrograph based on dispersing elements VPHG (Volume Phase Holographic Gratings) using fiber optic technologies. An electron-multiplying CCD-camera with high-speed image readout at minimal noise level (EMCCD) is used as the radiation receiver.

2.1 Methodology of photometric and spectral studies

The galaxies Mrk 6 and Mrk 1040 belong to the class of active galactic nuclei of the Narrow-Line Seyfert 1 galaxies (NLSy1), known as Seyfert galaxies (Table 1). This subclass of galaxies was discovered by Osterbrock and is characterized by narrow Balmer lines (Hβ line profile width less than 2000 km/s), intense FeII lines, and weak forbidden lines [7]. The methodology and processing of photometric observational data consist of standard operations using calibration Dark and Flat frames. Brightness measurements are conducted using the differential photometry methods (standard software package MaximDL Pro6). The stars with known brightness values in the vicinity of the object are selected as the standard stars (Table 2). To convert the obtained instrumental brightness estimates to the standard B V Rc system, corresponding transformation equations are applied [8].

Table 1. Seyfert galaxies for the study

Object	α(2000)	δ(2000)	V
Mrk 6 (IC450)	06 52 12.33	74 25 37.12	14.19
Mrk 1040 (NGC 931)	02 28 14.46	31 18 41.46	14.74

Table 2. Properties of standard stars for photometric studies

Object	Referent stars			
	Object	B	V	R
Mrk 6 (IC450)	GSC 04371-00113	15.06	14.44	14.33
Mrk 1040 (NGC 931)	Tycho-2323-1484-1	11.47	10.49	10.16

2.2 Methodology of Spectral Analysis

Accurate measurement of the velocity dispersion of broad components of spectral emission lines and their distribution plays a key role in estimating the masses of supermassive "black holes" in active galactic nuclei. Therefore, it is important to have an idea of the most accurate shape of the broad component profile, especially in the Hα region, where narrow components of the Hα and NII emission lines blend. To describe the shape of the profile, several separate components are used. However, in this case, the question arises of an adequate choice of the number of such components. For example, in [9], it is said that to correctly describe the line profiles, it was necessary to use several Gaussians. At the same time, the authors tried to use as few of them as possible, but at the same time they tried to ensure an adequate fitting of the observed line profiles. The criterion for adding additional components was a significant reduction in the root-mean-square error and χ2 during the fitting. This approach is somewhat subjective. The problem of determining the required number of components in the broad emission lines of Hα or Hβ can be solved within the concept of Bayesian analysis:

$$P(\Theta|D,M) = \frac{P(D|\Theta,M)P(\Theta|M)}{P(D|M)} \equiv \frac{L(\Theta)\pi(\Theta)}{Z} \quad , \tag{1}$$

where $P(\Theta|D,M)$ is the posterior (updated, taking into account the new data obtained) information (conditional probability) for the parameters Θ, taking into account the data D and the used model M. $P(D|\Theta,M) = L(\Theta)$ is the likelihood function (how probable the obtained data are, taking into account the chosen model and the its optimal parameters), $P(\Theta|M) = \pi(\Theta)$ is the prior (before the experiment, observations) probability for the parameters of the adopted model M, and $P(D|M) = Z$ is the marginal likelihood, otherwise called the model evidence, which is the integral over all possible model and parameter spaces. $P(D|M)$ determines the highest probability among all possible models:

$$P(D \mid M) \equiv Z \int_{\Omega_\theta} L(\Theta)\pi(\theta)d\Theta \tag{2}$$

It is clear that it is often not possible to estimate $P(D|M)$ (since we will need to consider all possible models and parameters for a given problem), but it can be used to estimate which of the models under consideration is more probable compared to other models. For the analysis of the spectra of Seyfert galaxies with the choice of the most probable model among the considered model (for example, in the case of different number of components in a wide profile), we use the nested sampling method [10], which, in addition to estimating the reliability of the model, gives us posterior distributions. The latter, in turn, can be used to estimate the model parameters and their error range:

$$\bar{\Theta}_i = E[\Theta_i] = \int \Theta_i P(\Theta_i \mid D,M)d\Theta_i \tag{3}$$

$$P(\Theta_i \mid D,M) \sim \int_{\forall\Theta_j \in (\Theta_j \neq \Theta_i)} L(\Theta_j)\pi(\Theta_j)d\Theta_j \tag{4}$$

To implement the nested sampling method, we use the DYNESTY package [11,12]. As prior information for each parameter in the model, we use a so-called 'non-informative' approach where the probability of values for the selected parameter is uniform over a range of accepted values (these constraints are known from previous studies of Seyfert galaxies). Unfortunately, this significantly increases computation time. However, in the future, this will allow us to analyze individual galaxies (or specific types of galaxies), using posterior information as prior for subsequent iterations (e.g., when new observational data is available). Additionally, in our models, we assume that the amplitudes in the [OIII] doublet are related by Aλ5007Å/Aλ4959Å = 2.99 [13] and the amplitudes in the [NII] doublet are related by Aλ6585Å/Aλ6550Å = 3.05 [14]. The widths of narrow emission lines are assumed to be identical (in terms of velocity dispersion) for all lines in the considered range, and the widths of broad profiles are also identical for all components of the broad emission spectrum. Doppler shifts of the 'red' and 'blue' components of the broad profile are also assumed to be identical (in the case of choosing a model with such components). To compensate for possible

.

errors in wavelength calibration, as well as inaccurate account of redshift, we introduce an additional parameter for each set of spectral lines. For precise determination of velocity dispersion values, we approximated the spectra with composite models. For the Hα region, these models consist of narrow emission lines of [OI], [SII], [NII] doublets, and the narrow Hα emission line, along with a broad Hα component. For the Hβ region, models include narrow emission lines of the [OIII] doublet and the narrow Hβ emission line, as well as a broad Hβ component. To complete the analysis, it is necessary to account for the stellar component of galaxies in both spectral regions. This can be achieved, for example, using the methodology implemented in the STARLIGHT package [15]. To incorporate the stellar contribution (continuum spectrum), we additionally included a power-law flux distribution in each composite model. In addition to approximating observed spectra with composite models to estimate parameters and analyze the broad components of Hα and Hβ, there is also the task of selecting the number of profiles (sub-components) in the broad Hα and Hβ profiles, as well as determining the shapes of the narrow emission line profiles. In our studies, we analyzed the result using both Gaussian profiles and profiles modeled as Voigt functions. The total number of parameters for the Hα region, using Voigt profiles for narrow components, three sub-components in the broad component of emission line Hα, and the additional assumptions mentioned earlier, was 18. For the Hβ region, the number of parameters was 14. For the model where all line profiles are described by Gaussians, the number of parameters was 17 and 13 respectively. Models with fewer broad emission line components (two or one) had fewer parameters.

3. Results of photometric and spectral analysis of the studied objects

MRK 6 (IC 450) is a Seyfert galaxy of the Sy1.0-1.5 class. Redshift z=0.018676±0.000834. The distance to the galaxy is 79 Mpc. The mass of the galaxy's central body (CB) is, MBH = (1-2)*10^8 Mc [16]. Active spectral and photometric studies of MRK 6 were carried out between 1990 and 2015 [17-20]. At FAI, MRK 6 observations in the BVRc photometric system have been carried out since 2016 [21]. Table A (Appendix) presents the results of photometric studies from November 25, 2019 to February 22, 2024. For general comparison, the results are presented as light curves (Figure 1) for the galaxy MRK 6 from 2016 to 2024.

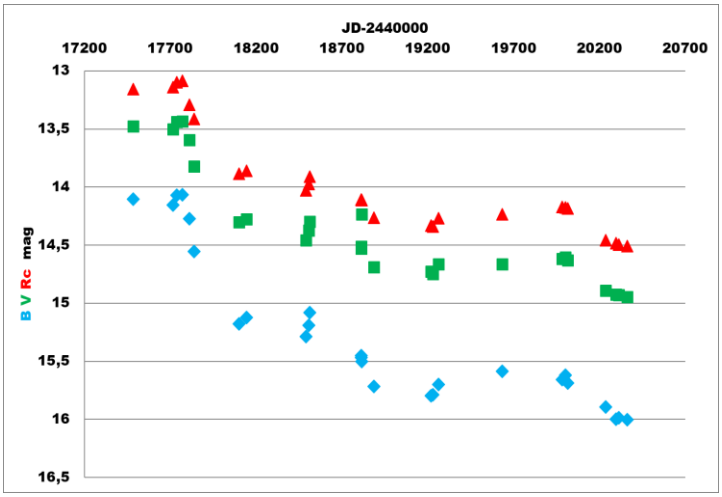

Fig.1. Light curves of MRK6 obtained in 2016-2024.
On the X-axis: Julian date - 2440000, and on the Y-axis: stellar magnitude

There was a unique opportunity to compare archival observational data with contemporary data over an extended time interval for the galaxy MRK 6. In previous works [22, 23] the digitization process and analysis of proprietary spectral data from the archive is described. In the spectra of MRK 6 obtained on February 4, 1976, on the left wing of the Hα line, an additional component is visible, shifted from the line center by 45 Å. Its radial velocity corresponds to 2450 km/s. In the spectra from 2023 and 2024, this detail appears in the Hα profile as a broad blue wing (Figure 2). Presumably, this additional component is created by a powerful jet (gas flow) moving towards the observer. Our modeling estimates indicated the radial velocity of this jet to be 2525^{+45}_{-49} km/sec (Figure 4). Additionally, a combined profile of the H_β region is presented (Figure 5), consisting of both narrow emission lines and profiles of the broad component.

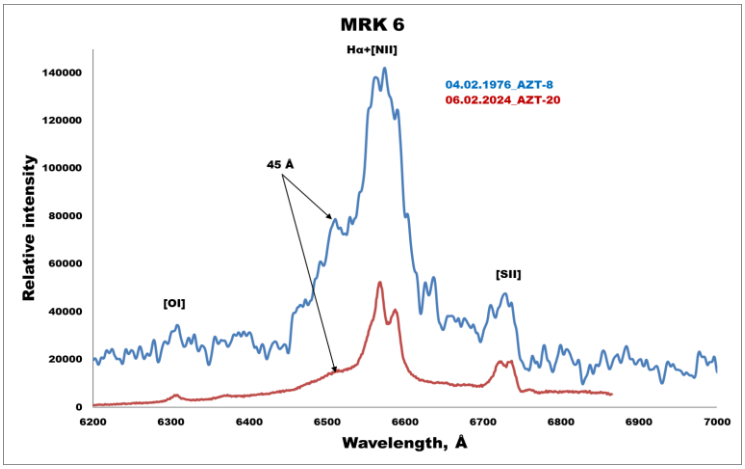

Fig. 2. Comparison of data obtained from digitizing archival spectra with results from 2024 (AZT-20)

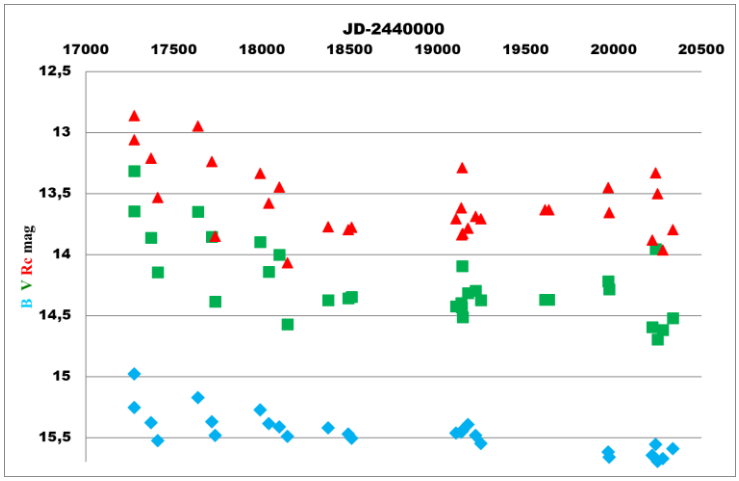

Fig.3. Light curves of MRK1040 obtained in 2015-2024. On the X-axis: Julian date - 2440000, and on the Y-axis: stellar magnitude.

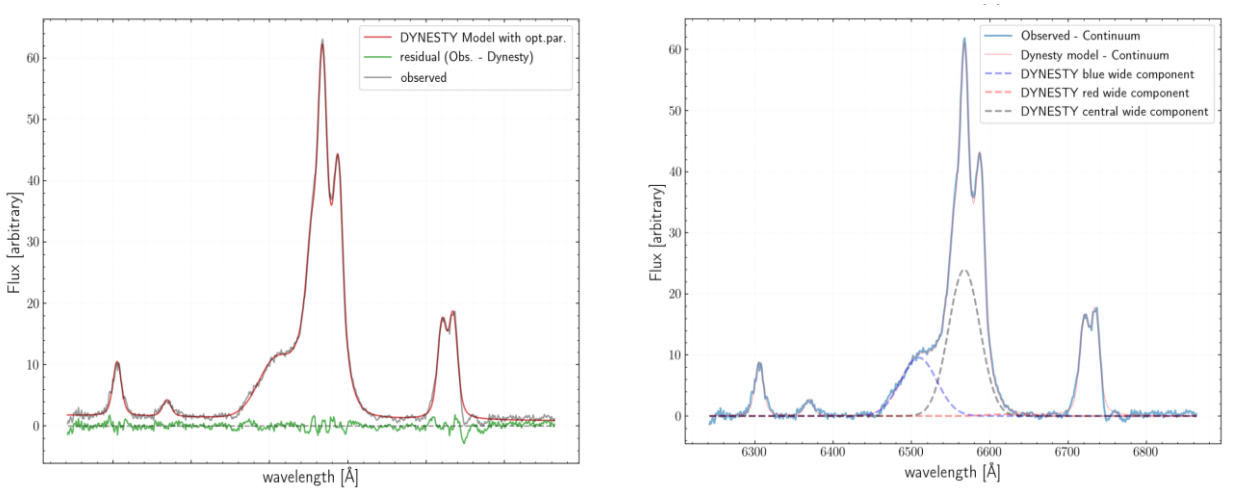

a) Hα, 3- component model b) Hα, 3- component model

Fig.4. The result of the model approximation with three components of the broad Hα line spectrum of MRK 6 obtained on AZT-20 06.02.2024

Table 3. The results of processing spectral data for the galaxy MRK6 obtained in 2023-2024

Emission line of the spectrum of Seyfert galaxies	λ (Å)	Continuum flux (erg s^{-1} cm^{-2} $Å^{-1}$)	Line flux (erg s^{-1} cm^{-2})	Equivalent width (Å)	Telescope
Mrk6 (16.01.2015)					
Hα+[NII]	6562	1.3E-14	5,562E-12	428	AZT-8
[SII]	6720	1.1E-14	2,44E-13	22	
Mrk6 (25.01.2023)					
[OI]	6300	6.284E-15	5.344E-14	8.498	AZT-20
Hα+[NII]	6562	9.102E-15	1.042E-12	111.8	
[SII]	6720	7.575E-15	1.909E-13	25.32	
Mrk6 (16.11.2023)					
Hα+[NII]	6562	1.083E-14	8.828E-13	81.98	AZT-20
[SII]	6720	7.035E-15	2.324E-13	33.55	
H_β	4861	1.363E-14	1.677E-13	12.31	
[OIII]	4959	1.039E-14	6.074E-13	58.33	
[OIII]	5007	1.178E-14	1.801E-12	149.5	
Mrk6 (06.02.2024)					
[OI]	6300	9.611E-15	1.405E-13	14.62	AZT-20
Hα+[NII]	6562	1.241E-14	3.258E-12	261.1	
[SII]	6720	1.229E-14	4.659E-13	38.24	
H_β	4861	2.712E-14	3.654E-13	13.49	
[OIII]	4959	2.678E-14	1.300E-12	48.46	
[OIII]	5007	2.678E-14	4.003E-12	148.3	

MRK 1040 (or NGC 931) is a bright Seyfert 1 spiral galaxy. It has a redshift of z=0.016338±0.000314 and is located at a distance of 340 Mpc. At FAI, photometric observations of MRK 1040 in the BVRc photometric system have been conducted since 2015 [21]. Table B (Appendix) presents the results of photometric studies from September 13, 2020, to January 27, 2024. For general comparison, the results are shown as light curves (Figure 4) for MRK 1040 from 2015 to 2024. The obtained data indicate that the studied object experiences irregular fluctuations in brightness in all three filters, with amplitudes of $B=0^m.337$, $V=0^m.874$, $R=0^m.734$.

The above-described spectral analysis methodology was applied to the spectral observations of the Seyfert galaxies MRK 1040 and MRK 6. Analysis of the spectra of MRK 6 obtained on February 6, 2024, showed that the model with three components of the broad Hα profile is more statistically significant compared to models with one or two components (Figure 4, Figure 6).

Table 4. The results of processing spectral data for the galaxy MRK 1040 obtained in 2023

Emission line of the spectrum of Seyfert galaxies	λ (Å)	Continuum flux (erg s^{-1} cm^{-2} $Å^{-1}$)	Line flux (erg s^{-1} cm^{-2})	Equivalent width (Å)	Telescope
MRK 1040 (20.01.2023)					
Hα+[NII]	6562	4.062E-15	7.211E-13	177.6	AZT-20
MRK 1040 (23.01.2023)					
Hα+[NII]	6562	4.007E-15	9.080E-13	225.6	AZT-20
MRK 1040 (25.01.2023)					
H_β	4861	2.810E-13	1.164E-11	41.42	AZT-20
[OIII]	4959	3.011E-13	1.664E-12	5.525	
[OIII]	5007	2.891E-13	5.921E-12	20.48	

As a result, we obtained the following velocity dispersion values for the narrow lines (NL) FWHM (NL) = 360^{+22}_{-22} $(km \cdot s^{-1})$ the line-of-sight velocity of the broad profile component 2525^{+45}_{-49} $(km \cdot s^{-1})$ and the velocity dispersion across the width of the broad central component of the lines (BL) FWHM (BL, central) = 1073^{+28}_{-29} $(km \cdot s^{-1})$ and components shifted relative to the central in the red and blue sides FWHM (BL, blue/red) = 1239^{+50}_{-45} $(km \cdot s^{-1})$ in the Hα region.

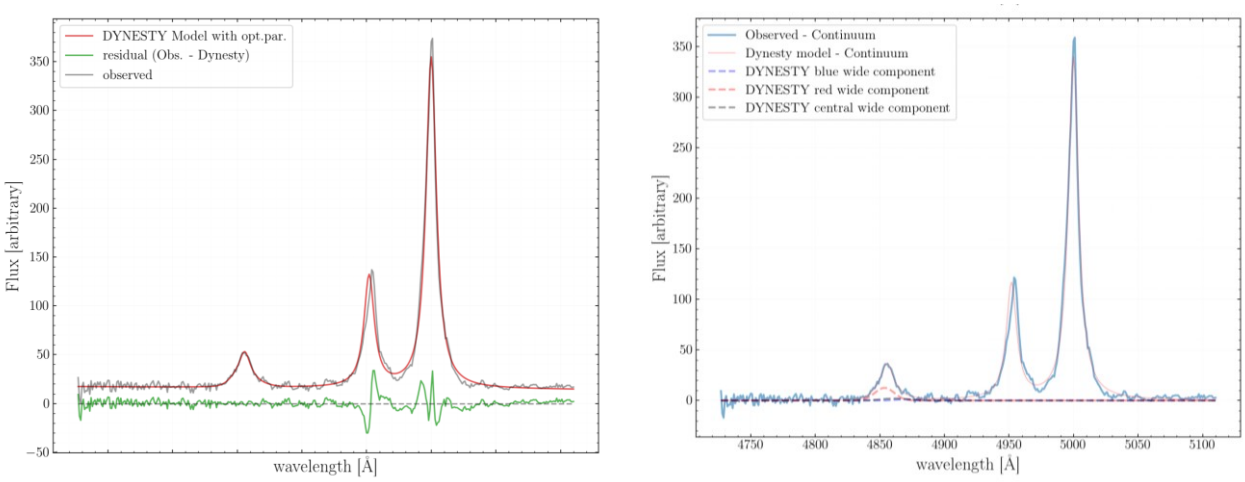

a) Hβ, 3-component model b) Hβ, 3-component model

Fig.5. The result of the model approximation of the broad H_β line spectrum of MRK 6 obtained on AZT-20 06.02.2024

Approximation of the Hβ region resulted in the velocity dispersion values for the narrow emission lines FWHM (NL) = $335^{+1.4}_{-1.0}$ $(km \cdot s^{-1})$, the line-of-sight velocity from the "blue" and "red" components of the broad profile 475^{+44}_{-62} $(km \cdot s^{-1})$. The velocity dispersion of the broad profile central component H_β FWHM (BL, central) = 1435^{+746}_{-271} $(km \cdot s^{-1})$ and the corresponding dispersion of the broad components profile H_β, shifted to the red and blue regions of the spectrum FWHM (BL, blue/red) = 1084^{+84}_{-57} $(km \cdot s^{-1})$.

The analysis of Mrk 1040 spectra obtained on January 21 and 23, 2023, showed that a model with a single component of the broad Hα profile is more statistically significant than models with more components (2 or 3) (Figure 6, Figure 7).

.

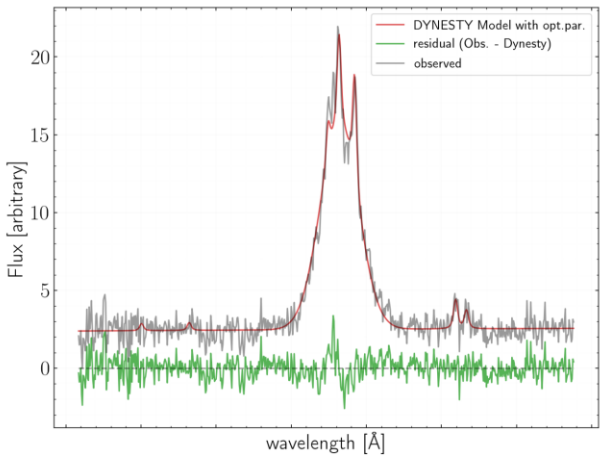

a) Hα, 1-component model

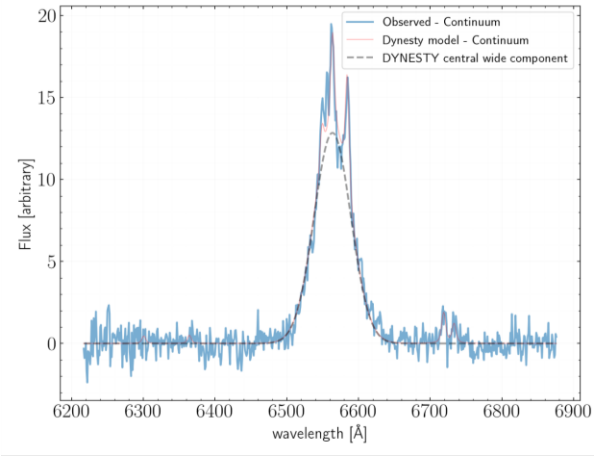

b) Hα, 1-component model

Fig.6. The result of the model approximation with one component of the broad Hα line spectrum of Mrk 1040 obtained on AZT-20 23.01.2023

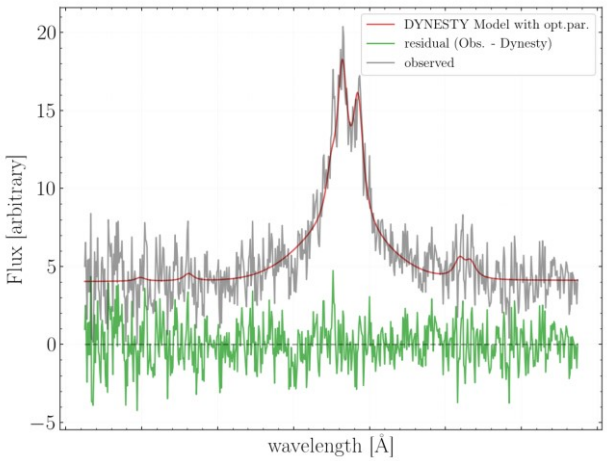

a) Hα, 1-component model

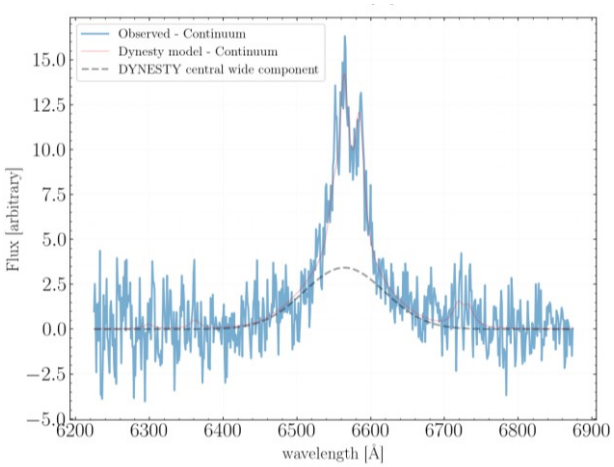

b) Hα, 1-component model

Fig.7. The result of the model approximation with one component of the broad Hα line spectrum of Mrk 1040 obtained on AZT-20 20.01.2023

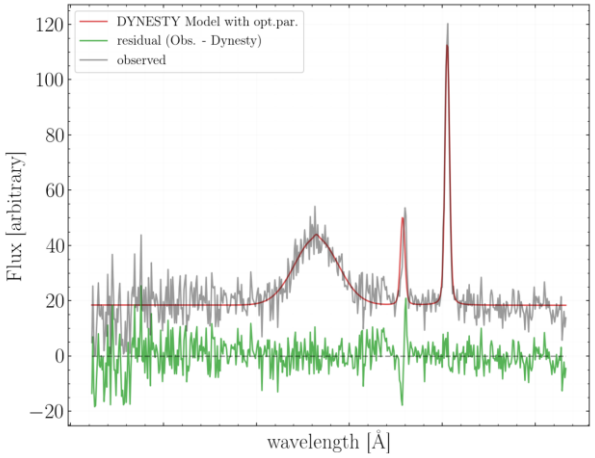

a) Hα, 1-component model

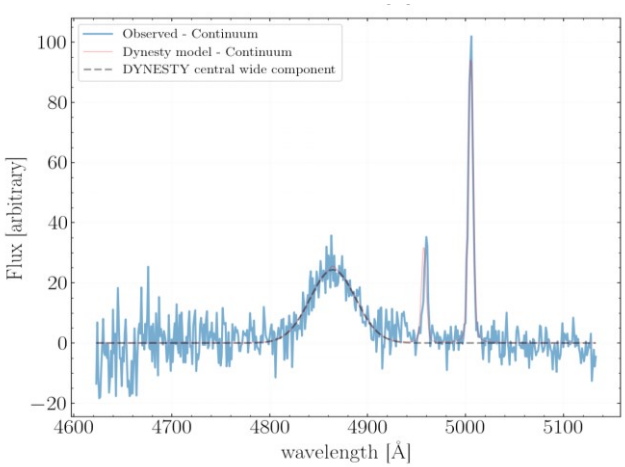

b) Hα, -component model

Fig.8. The result of the model approximation with one component of the broad Hβ line spectrum of Mrk 1040 obtained on AZT-20 25.01.2023

For Hα region approximation of the spectra taken on January 23, 2023, the velocity dispersion value for the narrow emission lines FWHM (NL) = 149^{+51}_{-63} $(km \cdot s^{-1})$. The velocity dispersion of the central component of the broad profile Hα FWHM (BL, central) = 1369^{+30}_{-28} $(km \cdot s^{-1})$.

For spectral data obtained on January 20, 2023, the approximation of the Hα region resulted in velocity dispersion value for the narrow emission lines FWHM (NL) = 52^{+46}_{-29} $(km \cdot s^{-1})$. The velocity dispersion of the central component of the broad profile Hα FWHM (BL, central) = 2950^{+284}_{-267} $(km \cdot s^{-1})$ (Figure 7).

The results of approximation of the Hβ region of the spectrum of Mrk1040 obtained on January 25, 2023, indicated that the broad Hβ profile was described by a single component (Figure 8). As a result of approximation the velocity dispersion value for the narrow emission lines FWHM (NL) = 232^{+5}_{-6} $(km \cdot s^{-1})$. The velocity dispersion of the central component of the broad profile H_β FWHM (BL, central) = 1695^{+20}_{-19} $(km \cdot s^{-1})$.

4. Conclusion

The paper presents new photometric and spectral data for galaxies from the Markarian list: Mrk 6 and Mrk 1040. Different research methods used by different scientists in the field of active galaxy nuclei are described. All the results obtained by other authors point to the complexity of the physical processes occurring in the studied objects. In the course of photometric studies of the galaxy Mrk 6, it was found that the brightness of this object for the period from 2016 to 2024 is unstable. The object reached its maximum luminosity in early 2017, and then by early 2018, its luminosity decreased by about ~1m. Since then, it has slowly continued to decrease. Observations of Mrk 1040 in the BVRc photometric system have been conducted since 2015. The data obtained show that the galaxy Mrk 1040 is subject to irregular light fluctuations in all three filters. The amplitudes of these oscillations are $B=0^m.337$, $V=0^m.874$, and $R=0^m.734$. Interestingly, spectrograms of the active nucleus of the Mrk 6 galaxy obtained on February 4, 1976, on the left wing of the Hα line showed an additional component displaced from the center of the line by 45 angstroms. Surprisingly, this component was also detected in the modern spectra obtained in 2024. Its radial velocity is 2450 km/s. Determining the number of components in broad spectral lines is a difficult task requiring a precise approach and taking into account many factors. Observations of spectra of active galactic nuclei are often difficult because of the overlap of different components. To adequately model such spectra, it is necessary to use methods capable of distinguishing and approximating individual components with high accuracy. Studies show that using several Gaussians to describe broad components of spectral lines can be an effective approach. However, it is important to keep in mind that the optimal number of components and their shape should be chosen taking into account the specifics of a particular observation and taking into account the statistical validity of the model. Methods of analyzing spectral data, such as Bayesian probability analysis and the nested sampling method, allow not only to determine the optimal number of components, but also to assess the reliability of the resulting model. This is important to avoid excessive model complexity or underestimation of the physical processes underlying the observed spectra. To determine the parameters of the Hα and Hβ region models and to analyze the broad components of Hα and Hβ, we recommend using the nested sampling method using the DYNESTY package. As a result of this method, we extracted narrow components of emission lines from the total spectrum, as well as broad components, the number of which was determined from an estimate of the relative statistical probability of a particular model. We determined the velocity dispersions for the components of the emission lines, as well as for the broad components of Hα and Hβ where detected, which may indicate the outflow of matter from the central regions of galaxies.

Conflict of interest statement
The authors declare that they have no conflict of interest in relation to this research, whether financial, personal, authorship or otherwise, that could affect the research and its results presented in this paper.

CRediT author statement
Shomshekova S.A.: Processing and analysis; Denissyuk E.K.: Processing; Kondratyeva L.N.: Observations; Serebryanskiy A.V.: Modeling; Aimanova G.K.& Aktay L.: Processing.
The final manuscript was read and approved by all authors.

.

Funding

This research is funded by the Science Committee of the Ministry of Education and Science of the Republic of Kazakhstan (Grant No. AP19676713) and by the Aerospace Committee of the Ministry of Digital Development, Innovations and Aerospace Industry of the Republic of Kazakhstan (Grant No. BR20381077).

Acknowledgements

We thank the FAI observers for their efficient work.

References

1 Layek N., Nandi P., Naik S., Kumari N., Jana A., Chhotaray B. (2024) Long-term X-ray temporal and spectral study of a Seyfert galaxy Mrk 6. *Monthly Notices of the Royal Astronomical Society,* 528 (3), 5269–5285. https://doi.org/10.48550/arXiv.2401.16780

2 Smirnova A.A., Moiseev A.V., Dodonov S.N. (2018) A close look at the well-known Seyfert galaxy: extended emission filaments in Mrk 6. *Monthly Notices of the Royal Astronomical Society,* 481 (4), 4542–4547. https://doi.org/10.1093/mnras/sty2569

3 Shablovinskaya E.S., Afanasiev V. L., Popović L.Č. (2020) Measuring the AGN Sublimation Radius with a New Approach: Reverberation Mapping of Broad Line Polarization. *The Astrophysical Journal,* 892, 2. https://doi.org/10.48550/arXiv.2003.12809

4 Pu Du, Michael S. Brotherton, Kai Wang, Zheng-Peng Huang, Chen Hu, David H. Kasper, William T. Chick, My L. Nguyen, Jaya Maithil, Derek Hand, Yan-Rong Li, Luis C. Ho, Jin-Ming Bai, Wei-Hao Bian, Jian-Min Wang (2018) Monitoring AGNs with Hβ Asymmetry. I. First Results:Velocity-resolved Reverberation Mapping. *The Astrophysical Journal,*869 (2), 17. https://doi.org/10.48550/arXiv.1810.11996

5 Nakhonthong N., Chainakun P., Luangtip W., Young A.J. (2024) Tracing the evolving X-ray reverberation lags within an individual AGN light curve. *Monthly Notices of the Royal Astronomical Society,* 530, 2. 1894-1906. https://doi.org/10.48550/arXiv.2404.04493

6 James Reeves, Valentina Braito, Ehud Behar, Travis Fischer, Steve Kraemer, Andrew Lobban, Emanuele Nardini, Delphine Porquet, Jane Turner. (2017) High-resolution X-Ray Spectroscopy of the Seyfert 1 Galaxy Mrk 1040. Revealing the Failed Nuclear Wind with Chandra. *The Astrophysical Journal,* 837, 1. 23. https://doi.org/10.48550/arXiv.1702.00461

7 Osterbrock D.E., Pogge R.W. (2017) The spectra of narrow-line Seyfert 1 galaxies. *The Astrophysical Journal*, 1985, 297, 166-176. https://doi.org/10.1086/163513

8 Shomshekova S. A., Reva I.V., Kondratyeva L.N. (2017) Standardization of the photometric system of the 1-meter telescope on TSHAO. *News of the National Academy of Sciences of the Republic of Kazakhstan Physico-Mathematical Series.* 4, 314, 155 – 161. Available to: https://journals.nauka-nanrk.kz/physics-mathematics/issue/view/225/252

9 Holden L.R., Tadhunter C.N., Morganti R., Oosterloo T. (2023) Precise physical conditions for the warm gas outflows in the nearby active galaxy IC 5063. *Monthly Notices of the Royal Astronomical Society,* 520, 2. 1848-1871. https://doi.org/10.1093/mnras/stad123

10 Skilling J. Nested Sampling. (2004). Bayesian Inference and Maximum Entropy Methods in Science and Engineering: Proceeding of the *24th International Workshop on Bayesian Inference and Maximum Entropy Methods in Science and Engineering,* 735. 395-405. https://doi.org/10.1063/1.1835238

11 Speagle J.S. (2020) DYNASTY: a dynamic nested sampling package for estimating Bayesian posteriors and evidence *Monthly Notices of the Royal Astronomical Society,* 493, 3. 3132-3158. https://doi.org/10.1093/mnras/staa278

12 Koposov S., Speagle J., Barbary K., Ashton G., Bennett E., Buchner J., Scheffler C., Cook D., Talbot C., Guillochon J., Cubillos P., Ramos A., Johnson B., Lang D., Dartiailh I.M., Nitz A., McCluskey A., Archibald A. (2023). *Josh speagle/dynasty:* 2.1.3 (v2.1.3). https://doi.org/10.5281/zenodo.8408702

13 Dimitrijević M.S., Popović L.Č., Kovačević J., Dačić M., Ilić D. (2007) The flux ratio of the [OIII] λλ5007, 4959 lines in AGN: comparison with theoretical calculations. *Monthly Notices of the Royal Astronomical Society,* 374, 3. 1181-1184. https://doi.org/10.1111/j.1365-2966.2006.11238.x

14 Dojčinović I., Kovačević-Dojčinović J., Popović L. Č. (2023) The flux ratio of the [N II] λλ 6548, 6583 Å lines in a sample of Active Galactic Nuclei Type 2. *Advances in Space Research*, 71, 2. 1219-1226. https://doi.org/10.1016/j.asr.2022.04.041

15 Cid Fernandes R., Mateus A., Sodré L., Stasińska G., Gomes J. M. (2005) Semi-empirical analysis of Sloan Digital Sky Survey galaxies - I. Spectral synthesis method. *Monthly Notices of the Royal Astronomical Society,* 358, 2. 363-378. https://doi.org/10.1111/j.1365-2966.2005.08752.x

16 Freitas I. C., Riffel R. A., Storchi-Bergmann T., Elvis M., Robinson A., Crenshaw D. M., Nagar N. M., Lena D., Schmitt H. R., Kraemer S. B. (2018) Outflows in the narrow-line region of bright Seyfert galaxies - I. GMOS-IFU data. *Monthly Notices of the Royal Astronomical Society,* 476, 2. 2760-2778. https://doi.org/10.1093/mnras/sty303

17 Granato G., Zitelli V., Bonoli F., Bonoli F., Danese L., Bonoli C., Delpino F. (1993) A Study of a homogeneous sample of optically selected Active Galactic Nuclei. III. Optical Observations *Astrophysical Journal Supplement,* 89, 35. https://doi.org/10.1086/191838

18 Doroshenko V., Sergeev S. (2003) Spectral activity of the Seyfert galaxy Markarian 6 in 1970-1991. *Astronomy & Astrophysics,* 405, 3. 909-915. https://doi.org/10.1051/0004-6361:20030587

19 Doroshenko V. (2003) Photometric activity of the Seyfert galaxy Markarian 6 from UBV observations in 1970-2001. *Astronomy & Astrophysics,* 405, 3. 903-908. https://doi.org/10.1051/0004-6361:20030586

20 Doroshenko V., Sergeev S., Klimanov S., Pronik V.I., Efimov Yu.S. (2012) Broad-line region kinematics and black hole mass in Markarian 6. *Monthly Notices of the Royal Astronomical Society*, 426, 1. 416-426. https://doi.org/10.1111/j.1365-2966.2012.20843.x

21 Shomshekova S., Denissyuk E., Valiullin R., Kusakin A., Reva I., Omarov Ch. (2019) Photometric Research of Seyfert Galaxies MRK 766, MRK 6, MRK 1040, MRK 1513. *News of the National Academy of Sciences of the Republic of Kazakhstan Physico-Mathematical Series.* 3, 325. 64-70. https://doi.org/10.32014/2019.2518-1726.25

22 Shomshekova S., Izmailova I., Umirbayeva A., Omarov C. (2022) A method for digitization of archival astro-plates of the Fesenkov Astrophysical Institute. *New Astronomy.* 97, 01881. https://doi.org/10.1016/j.newast.2022.101881

23 Shomshekova S., Kondratyeva L., Omarov Ch., Izmailova I., Umirbayeva A., Moshkina S. (2023) Digital archival spectral data for Seyfert galaxies and their use in conjunction with modern FAI spectral data. *Experimental Astronomy,* 56. 557–568. https://doi.org/10.1007/s10686-023-09916-6

AUTHORS' INFORMATION

Shomshekova, Saule Akhmetbekovna — PhD, Leading Researcher, Fesenkov Astrophysical Institute, Almaty, Kazakhstan; ORCID iD: 0000-0002-9841-453X; shmshekva-saule@mail.ru; shomshekova@fai.kz

Denissyuk, Eduard Konstantinovich — Candidate of Physical and Mathematical Sciences, Chief Researcher, Fesenkov Astrophysical Institute, Almaty, Kazakhstan; ORCID iD: 0000-0001-5020-2557; denissyuk@fai.kz

Kondratyeva, Ludmila Nikolaevna — Candidate of Physical and Mathematical Sciences, Chief Researcher, Fesenkov Astrophysical Institute, Almaty, Kazakhstan; ORCID iD: 0000-0002-6302-2851; kondratyeva@fai.kz

Serebryanskiy, Alexander Vladimirovich — PhD, Head of observational astrophysics department, Fesenkov Astrophysical Institute, Almaty, Kazakhstan; ORCID iD: 0000-0002-4313-7416; serebryanskiy@fai.kz

Aimanova, Gauhar Kopbaevna — Candidate of Physical and Mathematical Sciences, Chief Researcher, Fesenkov Astrophysical Institute, Almaty, Kazakhstan; ORCID iD: 0000-0002-3869-8913; gauhar@fai.kz

Aktay, Laura — Bachelor's, Engineer, Fesenkov Astrophysical Institute, Almaty, Kazakhstan; ORCID iD: 0009-0005-5862-4777; aktay@fai.kz

.

Appendix

Table A. B V R magnitudes for the galaxy MRK6 obtained in 2019-2024 Aperture 6”

Date of observations	JD-24400000	B	V	R
25.11.2019	18812	15,452	14,513	14,109
26.11.2019	18813	15,467	14,53	14,109
28.11.2019	18815	15,502	14,232	14,11
08.02.2020	18887	15,717	14,687	14,264
04.01.2021	19218	15,797	14,726	14,331
16.01.2021	19230	15,79	14,748	14,339
17.02.2021	19262	15,699	14,664	14,268
24.02.2022	19634	15,584	14,665	14,232
07.02.2023	19982	15,657	14,617	14,171
26.02.2023	20001	15,618	14,604	14,175
13.03.2023	20016	15,688	14,628	14,184
21.10.2023	20238	15,895	14,893	14,458
20.12.2023	20298	15,997	14,923	14,484
03.01.2024	20312	15,984	14,928	14,495
22.02.2024	20362	16,002	14,944	14,506

Table B. B V R magnitudes for the galaxy MRK1040 obtained in 2020-2024.Aperture 6,8”

Date of observations	JD	B	V	R
13.09.2020	19105	15,464	14,423	13,705
12.10.2020	19134	15,455	14,397	13,618
14.10.2020	19136	15,448	14,431	13,838
17.10.2020	19139	15,449	14,094	13,287
19.10.2020	19141	15,439	14,512	13,827
19.11.2020	19172	15,395	14,315	13,786
02.01.2021	19216	15,482	14,297	13,687
02.02.2021	19247	15,549	14,374	13,705
31.01.2022	19610	15,705	14,37	13,633
21.02.2022	19631	15,726	14,37	13,634
27.01.2023	19971	15,619	14,22	13,452
01.02.2023	19976	15,66	14,284	13,656
04.10.2023	20221	15,645	14,593	13,881
21.10.2023	20238	15,556	13,955	13,33
02.11.2023	20250	15,696	14,696	13,5
01.12.2023	20279	15,674	14,617	13,961
27.01.2024	20336	15,59	14,52	13,794